International Journal of Pharmaceutics 391 (2010) 79–89

Contents lists available at ScienceDirect

International Journal of Pharmaceutics

journal homepage: www.elsevier.com/locate/ijpharm

Construction and *in vitro* characterization of an optimized porosity-enabled amalgamated matrix for sustained transbuccal drug delivery

Oluwatoyin A. Adeleke, Viness Pillay*, Lisa C. du Toit, Yahya E. Choonara

Department of Pharmacy and Pharmacology, University of the Witwatersrand, 7 York Road, Parktown, 2193 Johannesburg, South Africa

ARTICLE INFO

Article history:
Received 21 June 2009
Received in revised form 10 February 2010
Accepted 11 February 2010
Available online 20 February 2010

Keywords:
Mechanistic characterization
Porosity-enabled amalgamated matrix
Transbuccal drug delivery
Experimental design
Simultaneous optimization

ABSTRACT

This research focused on constructing and characterizing an optimized porosity-enabled amalgamated matrix (P-EAM) for sustained transbuccal drug delivery. An interphase, co-particulate, co-solvent, homogenization technique and lyophilization guided through a Box–Behnken experimental design was employed in the fabrication, characterization and optimization of 15 P-EAMs. The effects of varying factor levels on the characteristic *in vitro* physicochemical performances of the P-EAMs were explored. Formulations had an average weight of 128.44 ± 3.48 mg with a dimensional size of 8 mm by 5 mm. Surface morphology showed varieties of pore structures, widespread distributions and uneven interconnectors. Satisfactory drug-loading was achieved (53.14 ± 2.19–99.02 ± 0.74%). Overall amount of drug released in 8 h was measured by the $MDT_{50\%}$ value which ranged between 22.50 and 225.00 min. Formulation demonstrated significant levels of *ex vivo* bioadhesive strength measured as detachment force (F_{det} = 0.964 ± 0.015 to 1.042 ± 0.025 N) and work of adhesion (ω_{adh} = 0.0014 ± 0.00005 to 0.0028 ± 0.00008 J). The potential of the P-EAMs to initiate and sustain *ex vivo* transbuccal permeation of drug was shown and measured as a cumulative value of between 25.02 ± 0.85 and 82.21 ± 0.57% in 8 h. Formulations were mesoporous in nature with pore sizes ranging from 40 to 100 Å characterized by the presence of interconnectors. Statistical constraints were simultaneously set to obtain levels of independent variables that optimized the P-EAM formulation.

1. Introduction

Porous matrices can be described as those possessing characteristic pore (hole) and interconnecting structures which have a significant influence on their performance. They have been studied over the years for their drug delivery applications and they continue to attract great research interest as they possess attractive features such as: (i) stable configuration, (ii) high surface area, (iii) flexible pore sizes, arranged in various distribution patterns, and (iv) defined surface properties, which are due to their unique porous structural configurations. They have found potential biomedical and drug delivery applications such as in the fabrication of biological tissue scaffolds (Kim et al., 2004; Sohier et al., 2006), implants (Moon Suk et al., 2005), hydrogels (Tang et al., 2005), ceramics (Netz et al., 2005; Miao et al., 2004; Rodríguez-Lorenzo and Ferreira, 2004), biocomposites (Wang et al., 2007), sponges (Portero et al., 2007), microcapsules (Chu et al., 2004), wafers (Bromberg et al., 2001; Matthews et al., 2005; Patel et al., 2007), membranes (Park et al., 1997; Åkerman et al., 1998), nanoparticles (Li et al., 2004) as well as in biomaterials engineering, life sciences and other relevant scientific spheres (Hoa et al., 2006). The above-mentioned qualities provide them with the potential to adsorb/load drug molecules and release them in a reproducible and predictable manner; enhance bio-adhesion to mucosal sites as well as augment permeation for the systemic delivery of drug molecules, which would be specifically useful for drug delivery via the transbuccal route, i.e. via the buccal mucosa (Sher et al., 2007; Zhang et al., 2007). In recent years, the demand for such sophisticated approaches for the delivery of therapeutic agents is on the increase (Tao and Desai, 2003). The particular focus on porous systems for transbuccal delivery lies in the potential use of these systems as inexpensive devices for the release of drugs at controlled, and perhaps time-independent rates. As investigated by Korsmeyer et al. (1983) for a hydrophilic porous system, progressive swelling of the polymer particles occur, emanating in considerable structural changes, which include alteration of the mobility of the macromolecular chains, macromolecular relaxations, and changes of the porous structure (e.g. alteration of the shape and size distribution of the pores). These ultimately impact on the porosity and tortuosity of the system during swelling and diffusional release. Finally, as swelling progresses, diffusion of the drug occurs both through the water-filled pores, and through the swollen polymer, which are influenced by the physical structure of the polymer, as well as the thermodynamic interactions between polymer and solute (Korsmeyer et al., 1983). Such a hydrophilic

* Corresponding author. Tel.: +27 11 717 2274; fax: +27 11 642 4355.
E-mail address: viness.pillay@wits.ac.za (V. Pillay).

0378-5173/$ – see front matter © 2010 Elsevier B.V. All rights reserved.
doi:10.1016/j.ijpharm.2010.02.023

system may provide favorable drug release owing to its porous nature.

Conventionally, drugs are delivered to the body employing the predominant routes of administration namely the oral route or injection. The use of injections (e.g. intravenous, intramuscular) which provides rapid physiological relief of symptoms is associated with a high level of pain during administration and may lead to high drug concentrations being released into the systemic circulation which can be fatal. The oral route of drug delivery on the other hand offers several advantages, namely that it is more acceptable, less invasive and can be painlessly self-administered (Tao and Desai, 2003). However, research has shown that after oral administration, many drugs are subject to extensive pre-systemic elimination by gastrointestinal degradation and/or hepatic first pass metabolism as well as resistance exerted by the intestine that may result in low systemic bioavailability, short duration of therapeutic activity and/or formation of inactive or toxic metabolites (Ponchel et al., 1997; Ahmed et al., 2002; Orive et al., 2003; Sudhakar et al., 2006). In order to circumvent some of the above-mentioned limitations associated with the oral and injection routes of drug administration, transmucosal drug delivery has been explored as an alternative route of administering drugs (Smart, 2005; Chien, 2006; Sudhakar et al., 2006). It offers the potential for the non-invasive, regulated systemic absorption of drugs and may serve as useful sites with good accessibility for easy application of drug delivery systems (Chien, 2006).

This investigation employed the buccal mucosa as a model for transmucosal drug delivery because among the various sites, it is most suitable for administration of retentive dosage forms. This is due to its excellent accessibility for self-administration, short recovery times after stress or damage, rich blood supply, an expanse of smooth muscle, direct access to the systemic circulation which allows drugs to bypass the pre-systemic metabolic processes thus leading to an increased bioavailability and rapid onset of action. Other advantages include painless administration, versatility and simplicity, easy drug withdrawal whenever desired and the ability to include permeation enhancers, enzyme inhibitors, pH modifiers or bioadhesive compounds and other pharmaceutical additives in the formulation for local or systemic actions (Alur et al., 2001; Sudhakar et al., 2006).

The present study focuses on the construction and optimization of a novel bioadhesive porosity-enabled amalgamated matrix (P-EAM) for sustained drug release *via* the transbuccal route into the systemic circulation employing phenytoin sodium as a model drug. Phenytoin sodium is widely utilized as a first-line drug in the effective treatment of epilepsy worldwide. It possesses relatively slow rates of systemic absorption (Darwish et al., 1996; Alvarez-Nύñez and Yalkowsky, 1999; Wang and Patsalos, 2003; Pellock et al., 2004). Phenytoin sodium has been reported to exhibit a high dissolution rate in water but under gastrointestinal acidic pH conditions, the sodium salt is rapidly converted to the practically insoluble acid form which may have some influence on its bioavailability (Darwish et al., 1996). Consequently, a need exists to design an optimized drug delivery system with potential capabilities to overcome the reported demerits of phenytoin sodium.

As far as we know, inadequate explorative studies exist relating to the construction, mechanistic characterization, and optimization of novel porosity-enabled systems which may be described as superior to conventional formulations employed for controlled systemic drug delivery through the buccal transmucosal site. In order to construct the porosity-enabled amalgamated matrix, an interphase, co-particulate, co-solvent, homogenization technique coupled with lyophilization were utilized. The choice of method of preparation was based on its simplicity and optimum efficiency in generating robust and stable formulations which would enable an undemanding industrial process operation and minimized production cost, enhancing patient affordability. The construction of the unique matrices was guided through a high performance statistically and mathematically robust experimental design approach. Relevant physicochemical characterizations, which involved determination of formulation weight, *in vitro* drug release behaviour, drug loading capacity, *ex vivo* bioadhesive strength, rheological assessments, surface morphology, *ex vivo* permeation efficiency, quantitative evaluation of matrix porosity and elucidation of physical or chemical transitions were performed.

2. Materials and methods

2.1. Materials

Chitosan (CHT) (food grade) and menthol (MTH) were purchased from Warren Chem Specialties, Johannesburg, South Africa. Gelatin (GEL), phenytoin sodium (PS-Na), polyvinyl alcohol (PVA) (molecular weight = 72,000 g/mol) and magnesium stearate (MS), were purchased from Sigma Chemical Company (St. Louis, USA). Span® 80 (Sorbitan ester 80) (SP 80) and ethanol (EtOH) (95%) were procured from Merck Chemicals (Darmstadt, Germany) and Saarchem (Johannesburg, Gauteng, South Africa), respectively. Carbopol® 974P NF (CARB) was acquired from Noveon, Inc., (Cleveland, Ohio, USA). Ethylcellulose (Ethocel® 10) (ETH) was obtained from Protea Industrial Chemicals (Pty) Ltd. (Wadesville, South Africa). Hydroxyethylcellulose (HHX 250 Pharm) (HEC) was purchased from Hercules, Aqualon (Germany). All other reagents utilized were of analytical grade and used as received.

2.2. Preparation of the porosity-enabled amalgamated matrices (P-EAM) in accordance with a Box–Behnken experimental design template

Fifteen P-EAMs were prepared using various combinations of independent variables by the processes of interphase homogenization and lyophilization guided through a three factor, and three centre points Box–Behnken quadratic design using Minitab Statistical Software, Version 14 (Minitab Inc., State College, PA, USA). Three categories of independent variables composed of the solutes, solvents and surfactant, Span 80 were employed in fabricating the P-EAMs and were based on statistically and mathematically generated Box–Behnken design template and these included:

(i) Aqua-based co-particulate dispersion (ACD) composed of PVA, HEC, CARB, GEL and DW.
(ii) Ethanol-based co-particulate dispersion (ECD) composed of ETH, MS, MTH, CHTS and EtOH.
(iii) Span® 80 (SP 80) only.

Tables 1 and 2 present the levels of the independent variables employed and the experimental design template for the 3 factors, 3 centre points and 15 experimental runs, respectively. The lower and upper limits for the factors were set based on their ability to

Table 1
Levels of the independent variables employed in the Box–Behnken design template.

Independent variables	Levels		Units
	Low	High	
ACD[a]	0	2	mg/20, 25 or 30 mL
ECD[b]	3	5	mg/13, 11 or 7 mL
SP 80[c]	0.3	0.7	mL

[a] Aqua-based co-particulate dispersion.
[b] Ethanol-based co-particulate dispersion.
[c] Span 80.

Table 2
Box–Behnken design template for the preparation of each porosity-enabled amalgamated matrix.

Formulation	Composition		
	ACD (mg/20, 25 or 30 mL) [a]	ECD (mg/13, 11 or 7 mL) [b]	SP 80 (mL) [c]
1	0	5	0.5
2	0	3	0.5
3[d]	1	4	0.5
4	0	4	0.7
5[d]	1	4	0.5
6	1	3	0.3
7	1	5	0.7
8	2	3	0.5
9	1	5	0.7
10	2	4	0.3
11[d]	1	4	0.5
12	2	5	0.5
13	2	4	0.7
14	1	5	0.3
15	0	4	0.3

Note: ACD: 0 – PVA (800 mg) + HEC (350 mg) + GEL (400 mg) + CARB974 (100 mg) + DW (30 mL); 1 – PVA (475 mg) + HEC (525 mg) + GEL (350 mg) + CARB974 (150 mg) + DW (25 mL); 2 – PVA (300 mg) + HEC (700 mg) + GEL (300 mg) + CARB974 (200 mg) + DW (20 mL).
ECD: 3 – CHTS (550 mg) + MS (350 mg) + MTH (200 mg) + ETH 10 (400 mg) + EtOH (13 mL); 4 – CHTS (425 mg) + MS (325 mg) + MTH (250 mg) + ETH 10 (500 mg) + EtOH (11 mL); 5 – CHTS (300 mg) + MS (300 mg) + MTH (300 mg) + ETH 10 (600 mg) + EtOH (7 mL).

[a] Aqua-based co-particulate dispersion.
[b] Ethanol-based co-particulate dispersion.
[c] Span 80.
[d] Centre points for the experimental design template.

form stable, robust drug-loaded P-EAMs using minimal quantities of the individual components.

The P-EAMs were produced using various quantities of ACD, ECB and SP 80 described earlier by the process of interphase co-particulate, co-solvent homogenization. The combinations of both polymeric and non-polymeric solutes, ACD and ECD, were separately dispersed in two polar protic solvents, water and ethanol, respectively. Each matrix contained 50 mg phenytoin sodium which was dispersed in the water-based medium (ACD). The two dispersions were mixed and specific quantities of SP 80 were used to reduce the surface tension of the solutes and solvents to enhance homogenization to form a stable blend. Overall, the formation of the homogenous blend was aided with a laboratory scale homogenizer (Polytron® 2000, Kinematica AG, Switzerland) for 10 min. The resulting blend was then cured for 30 min in the dark to enhance solute–solvent physical intermolecular interactions to occur. For each P-EAM, 1.0 mL of the blend produced was pipetted into specialized, pre-oiled (employing inert liquid paraffin) polystyrene moulds (10 mm diameter × 10 mm height). Formulations were pre-frozen at −72 °C for 24 h and then subjected to lyophilization by placing them into a freeze dryer (Bench Top 2K, Virtis, New York, USA) set at −55 ± 2 °C and 0.42 mBar for 48 h. Post lyophilization, produced P-EAMs were stored for further testing in closed glass jar with active silica-containing desiccant bags.

2.3. Evaluation of the drug release behaviour

Drug release studies were conducted by immersing each formulation into 25 mL of simulated saliva (pH 6.8) contained in closed 100 mL capacity glass jars. For studies at the specified conditions, three replicate samples of the individual matrices were maintained at 37 ± 0.5 °C and 20 rpm in a shaking incubator (Orbital Shaker Incubator, LM-530, Lasec Scientific Equipment, Johannesburg, South Africa). 3 mL dissolution samples were manually withdrawn at specific time intervals (30, 60, 120, 240, 360, and 480 min) over 8 h and filtered through a 0.45 μm pore size Cameo Acetate membrane filter (Milipore Co., Bedford, MA). Sink conditions were maintained by replacing withdrawn volume with fresh simulated saliva at each sampling time. The amount of phenytoin sodium released was determined utilizing a ultraviolet spectrophotometer (Cecil CE 3021, 3000 Series, Cecil Instruments, Cambridge, England) at λ_{max} = 206 nm.

2.4. Surface morphological characterization of the P-EAMs

In addition, the nature and architecture of the porous surface morphology of each formulation was visualized and characterized using scanning electron microscopy (SEM). Samples (8 mm diameter × 5 mm thickness) were sputter-coated with gold–palladium and viewed four times from different angles under a JSM-840 scanning electron microscope (JEOL 840, Tokyo, Japan) at a voltage of 20 keV and a magnification of 1000×.

2.5. Computation of the percentage drug-loading capacity

The percentage drug-loading capacity (% DLC) was calculated using Eq. (1). This parameter was an indication of the drug loading efficiency of the P-EAMs.

$$\%\text{DLC} = \frac{A_d}{T_d} \times 100 \quad (1)$$

where % DLC: percentage drug-loading capacity, A_d: actual amount of drug loaded and T_d: theoretical amount of drug loaded.

For each determination, one P-EAM was completely dissolved in 100 mL simulated saliva solution (pH 6.8) with the aid of the laboratory homogenizer (Polytron® 2000, Kinematica AG, Switzerland). 2 mL sample was then manually withdrawn and filtered through a 0.45 μm pore size Cameo Acetate membrane filter (Milipore Co., Bedford, MA). Appropriate dilutions were carried out and samples were then analyzed utilizing the ultraviolet spectrophotometer (Cecil CE 3021, 3000 Series, Cecil Instruments, Cambridge, England) at 206 nm. The absorbance values generated were fitted with the linear equation ($y = 16.516x$; $R^2 = 0.995$) of the calibration curve obtained for phenytoin sodium. The outcome of this computation was then substituted into Eq. (1) above to generate the %DLC for each formulation. All evaluations were conducted in triplicate.

2.6. Ex vivo permeation studies utilizing the porcine buccal mucosa

2.6.1. Tissue collection and preservation

The porcine buccal mucosa was obtained from the cheek region of freshly slaughtered domestic pigs. After collecting the mucosal specimens, they were immediately transported in a refrigerated transport box and transferred to our *in vivo* laboratory within 1 h. The pig's buccal mucosa was specifically selected for this study because they have non-keratinized buccal mucosa similar to that of human beings. In fact, the oral mucosa of pigs resembles that of humans more closely than any other animal in terms of structure and composition (Sudhakar et al., 2006).

Excess connective and adipose tissues were trimmed away (using surgical scalpel and scissors) from the harvested buccal mucosal specimens. The average porcine buccal mucosal thickness employed throughout the study was 0.9 ± 0.1 mm. This was measured using digital vernier caliper (25 mm × 0.01 mm capacity, Germany). Subsequently, the trimmed specimens were snap frozen in liquid nitrogen and stored at −70 °C for up to 2 months. Researchers have reported that freezing tissue specimens (either snap freezing with liquid nitrogen or in a standard freezer) does not change their diffusion or permeation behaviour when used for such studies (Van der Bijl et al., 1998; Van Eyk and Thompson, 1998;

Van Eyk and Van der Bijl, 2004; Consuelo et al., 2005; Giannola et al., 2007).

2.6.2. Preparation of tissue and permeation studies

Before conducting each permeation experiment, the frozen buccal mucosal specimens were thawed and re-hydrated to regain elasticity temporarily lost when frozen for 2 h in 100 mL phosphate buffered saline (PBS, pH 7.4) at room temperature (21 ± 0.5 °C). The PBS solution was changed every 30 min with a fresh solution. After re-hydration, mucosal disks (diameter = 15 mm and surface area = 2.27 cm^2) were cut using surgical scissors from the harvested specimen and mounted in the flow through Franz-type diffusion cell apparatus (Membrane transport systems, V3, Permegear, Amie Systems, USA) connected to a heat-circulating water bath/heating system (CPE 100, Labcon, Maraisburg, Gauteng, South Africa). The receiver compartment contained 10 mL simulated plasma, pH 7.4 (Giannola et al., 2007) while the donor compartment contained a 2 mL solution of the drug-loaded P-EAM formulation in simulated saliva, pH 6.8 (Peh and Wong, 1999). Uniform mixing within the receiver compartment was achieved by magnetic stirring. Permeation studies were conducted in triplicate for each formulation at 37 ± 0.5 °C. At pre-determined time intervals over 480 min (30, 60, 120, 240, 360, 480 min), 2 mL sample volume was withdrawn from the receiver compartment of each cell and replaced with the same volume of fresh simulated plasma. Withdrawn samples were assayed for phenytoin sodium at 206 nm on a Cecil CE 3021, 3000 Series (Cecil Instruments, Cambridge, England).

The drug flux values (J_s), through the membrane, were calculated at the steady state per unit area by linear regression analysis of permeation data following Eq. (2) (Giannola et al., 2007).

$$J_s = \frac{Q_r}{A \times t} \quad (2)$$

where J_s is the drug flux (mg cm^{-2} min^{-1}), Q_r is the amount of phenytoin sodium that passed through the porcine buccal mucosa into the receptor compartment (mg), A is the active cross-sectional area accessible for diffusion (cm^2) and t is the time of exposure in minutes.

2.7. Ex vivo assessment of bioadhesive capacity using porcine buccal mucosa

The *ex vivo* bioadhesive strength of the P-EAMs were determined using a calibrated Texture Analyzer (TA.*XTplus*, Stable Microsystems, Surrey, England) fitted with a cylindrical stainless steel probe (10 mm diameter) and freshly isolated porcine buccal mucosa (0.8 ± 0.1 mm thickness) as the model tissue. All measurements were performed in triplicate. The buccal mucosa was attached to the cylindrical probe while the P-EAM was mounted onto the texture analyzer stage. The two surfaces were aligned to ensure that they came into direct contact with each other during measurements. The settings employed during testing were: contact force (0.1 g), pre-test speed (2 mm/s), test speed (0.5 mm/s), post-test speed (10 mm/s), applied force (1 N), return distance (8 mm), contact time (10 s), trigger type (auto) and trigger force (0.049 N). For each measurement, the surface of the porcine buccal mucosa was made evenly wet by soaking into 2 mL simulated saliva placed in a glass petri dish for 5 min. Subsequently, the tissue was lowered towards the formulation on the stage to make contact. Bioadhesive strength was calculated from the generated force–distance curve as the peak detachment force (F_{det}) measured in Newton (N) and work of adhesion (ω_{adh}) in Joule (J). The peak detachment force was taken as the maximum force needed for detaching the matrix from the tissue while the work of adhesion was calculated as the area under the force–distance curve.

2.8. Quantitative porositometric analysis

Porosimetry is an analytical technique used to determine various quantifiable aspects of a material's porous nature such as total pore volume, surface area and average pore diameter which provides information about pore types. These parameters were detected in triplicate using a surface area and porosity analyzer equipped with the ASAP 2020 V3.01 software (Micromeritics, ASAP 2020, Norcross, GA, USA). A dry sample weight of 130 ± 10 mg was employed for all 15 formulations. The porosimetric investigations were conducted in two phases, degassing and analysis stages. Samples were subjected to degassing to remove air, gases and other adsorbed species from the sample surface. The operating settings employed included temperature ramp rate (10 °C/min), target temperature (30 °C), evacuation rate (50 mmHg/s), unrestricted evacuation (30 mmHg), vacuum set point (500 μmHg), evacuation time (60 min), heating hold temperature (20 °C), hold time (900 min), evacuation and heating hold pressure (100 mmHg) and analysis time (400 min).

2.9. Constrained statistical optimization

The primary aim of this statistical process was to develop an optimal P-EAM for sustained release, systemic transbuccal drug delivery applications. After generating the quadratic polynomial regressions from the Box–Behnken design template which related the independent to the dependent variables, experimental results were fitted within set constraints for predicting the optimal formulation. A simultaneous optimization approach was performed using the response surface optimizer function on the software (Minitab Software, Version 14, USA). With this technique, constraints were set to obtain levels of independent variables that simultaneously manipulated the relevant response parameters or dependent variables to the desired statistically optimal levels. Consequently, a target level was set for the mean dissolution time (indicative of drug release behaviour) while the drug-loading capacity, bioadhesion, and cumulative drug permeation were maximized with respect to the desired release behaviour. With regards to the purpose of this constrained optimization process, the response parameters, mean dissolution time, drug-loading capacity, bioadhesion, and cumulative drug permeation, were set at different levels (Table 3). The above-mentioned response parameters were selected for optimization purposes as they are a function of all measured physicochemical parameters which have been noted to influence the overall performance of the P-EAM to suit its intended application. A desirability function, a value that measures the accuracy of the statistical process, of 0.96 was obtained.

A one-way analysis of variance (ANOVA) was applied to estimate the significance and reliability of the statistical model. The response parameters employed above were also chosen for the simultaneous optimization process because of the correlation measures that were employed to estimate the fitness of the statistical model for accurate prediction. The model-dependent terms employed in this study included the: (i) *p-values* set at 95% confidence level ($p < 0.05$ *were considered as statistically significant*) and (ii) the correlation coefficient, R^2 (set at values greater than 0.90 because of the com-

Table 3
Numerical targets set for the selected response parameters.

Parameters	Statistical goal	Lower	Target	Upper
Mean dissolution time (MDT) (min)	Target	80.00	90.00	100.00
Drug loading capacity (DLC) (%)	Maximum	90.00	100.00	100.00
Bioadhesive strength (BA) (Newton)	Maximum	1.10	1.20	1.20
Cumulative drug permeation (PA) (%)	Maximum	80.00	90.00	90.00

Table 4
Levels of statistical significance of the response parameters employing ANOVA.

Response parameters	*p*-Values	R^2
Mean dissolution time	0.031	0.907
Drug loading capacity	0.013	0.948
Bioadhesive strength	0.048	0.905
Cumulative drug permeation	0.011	0.991

plexities of the quadratic experimental design approach). Table 4 outlines the levels of significance for the response parameters.

3. Results and discussion

3.1. Physical appearance and weight variability of the P-EAMs

Generally, the P-EAMs appeared as whitish, compact, semi-circular platforms with a diameter of 8 mm and thickness of 5 mm. Overall the matrices had gravimetric weights ranging from lowest (121.95 ± 0.95 mg) to highest (133.75 ± 0.35 mg) and an average weight of 128.44 ± 3.49 mg for all the 15 formulations. The differences in weights exhibited by the 15 formulations are attributable to the differences in the quantities of the components (both solute and solvent levels) employed in the fabrication of each set of formulation. As regards intra-formulation weight differences, a close relationship ($r = 0.961$) existed amongst each set of matrices prepared from the same formulation. Consequently, it can be proposed that the interphase, co-particulate, co-solvent, homogenization technique utilized in preparing the porous matrices was efficient and produced a homogenous blend which minimized disparities within the P-EAM formulation batches.

3.2. Drug release from the matrices

Diverse release patterns were observed for the 15 formulations which may be associated with the various degrees of co-particulate dispersion, interphase homogenization, solute–solvent interaction and lyophilization due to the differences in the quantities of the constituents utilized in fabricating each formulation (Table 2). Fig. 1 illustrates the drug release trends exhibited by the 15 formulations.

The diverse dissolution patterns displayed by the 15 formulations were analyzed and substantiated by the time-point approach referred to as mean dissolution time (MDT). The application of the MDT provides a more accurate view of the drug release behaviour as it is determined as the sum of the individual periods of time during which a specific fraction of the total drug dose is released (Pillay and Fassihi, 1998; Rinaki et al., 2003). Eq. (3) was employed in the calculation of the MDT.

$$\mathrm{MDT} = \sum_{i=1}^{n} t_i \frac{M_t}{M_\infty} \quad (3)$$

where M_t is the fraction of dose released in time t_i, $t_i = (t_i + t_{i-1})/2$ and M_∞ corresponds to the loading dose.

The $\mathrm{MDT}_{50\%}$ data point was selected for the 15 formulations as this was applicable to all generated profiles (Fig. 2). The $\mathrm{MDT}_{50\%}$ numerical values are stated in Table 5. Low $\mathrm{MDT}_{50\%}$ and high $\mathrm{MDT}_{50\%}$ values represent rapid or prolonged/controlled drug release patterns, respectively.

All the 15 formulations elicited variable levels of burst release of drug at $t_{30\,\mathrm{min}}$ and this may be attributable to their diverse porous nature (Fig. 1). This initial relatively rapid liberation of drug molecules was followed by a moderately consistent release trend over time. The observed trend may be of advantage to the intended application of this drug delivery system as the initial burst release initiates the pharmacological action which is sustained by the consistent release of drug molecules over time. The P-EAMs

Table 5
$\mathrm{MDT}_{50\%}$ values depicting the drug release characteristics of the formulations.

Formulation	$\mathrm{MDT}_{50\%}$ (min)
1	104.00
2	85.00
3	98.00
4	105.00
5	104.50
6	220.00
7	225.00
8	88.50
9	15.00
10	185.00
11	100.00
12	210.00
13	90.00
14	161.00
15	22.50

demonstrated the potential for application as a controlled release system over 8 h. The levels of both hydrophilic and hydrophobic co-particulate component contained in each formulation appeared to have noticeable complex effects on the drug release pattern.

Generally, formulations comprised of higher levels of hydrophobic solutes than the hydrophilic components displayed a more controlled release pattern while the reverse was observed for those containing higher levels of the hydrophilic components than the hydrophobic solutes. Exceptions to this trend were also observed. Furthermore, the quantities of the pore-forming agents, water and ethanol, appeared to influence the drug release behaviour of the formulations. This may be attributable to the susceptibility of the frozen, solidified (due to the pre-freezing of the homogenous blend) individual pore-forming agent to sublimation during the process of lyophilization due to their individual densities (ethanol = 0.70 g/mL and water 1.00 g/mL). Consequently, ethanol molecules which are less dense than water, may be converted to gas more rapidly during the process of lyophilization thereby forming a more spacious/open porous network as compared to water, its denser counterpart producing a more closely knitted porous structure. Overall, the differences in their pore-forming capacities can influence the processes of water influx, hydration and matrix disentangling which may then influence the exhibited drug release behaviour of each formulation.

3.3. Surface morphological characterization of the P-EAMs

Scanning electron microscopy revealed the variety of pore structures, distributions and interconnectors embedded within the sets of P-EAM matrices. Their surface porous configuration was rather complex, irregular and extensive (Fig. 2). Generally, the kinds of pore structures observed ranged from circular (Fig. 2b, c, e, h, k, m and o) to those with asymmetrical geometries (Fig. 2a, d, f, g, i, j, l and n). The pores were comparatively widespread throughout the surfaces of each matrix. The interconnectors, which can be described as barriers or partitions that demarcate the pores, were rather uneven and were described as either rigid (Fig. 2f, g, j and n), web-like/thread-like (Fig. 2b, c, e, h, k, m and o) or spongy (Fig. 2a, d and i) in structure.

Furthermore, a relationship between the surface morphology and the drug release characteristics of the matrices was observed. It was observed that the pore interconnectors played a noticeable role in their drug release performances. Matrices with web-like, thread-like and spongy interconnectors (Fig. 2a, b, c, d, e, h, i, k, m, and o representing formulations 1, 2, 3, 4, 5, 8, 9, 11, 13 and 15) demonstrated quicker but controlled release rates with over 65% drug released within 8 h (Fig. 1). The converse was observed

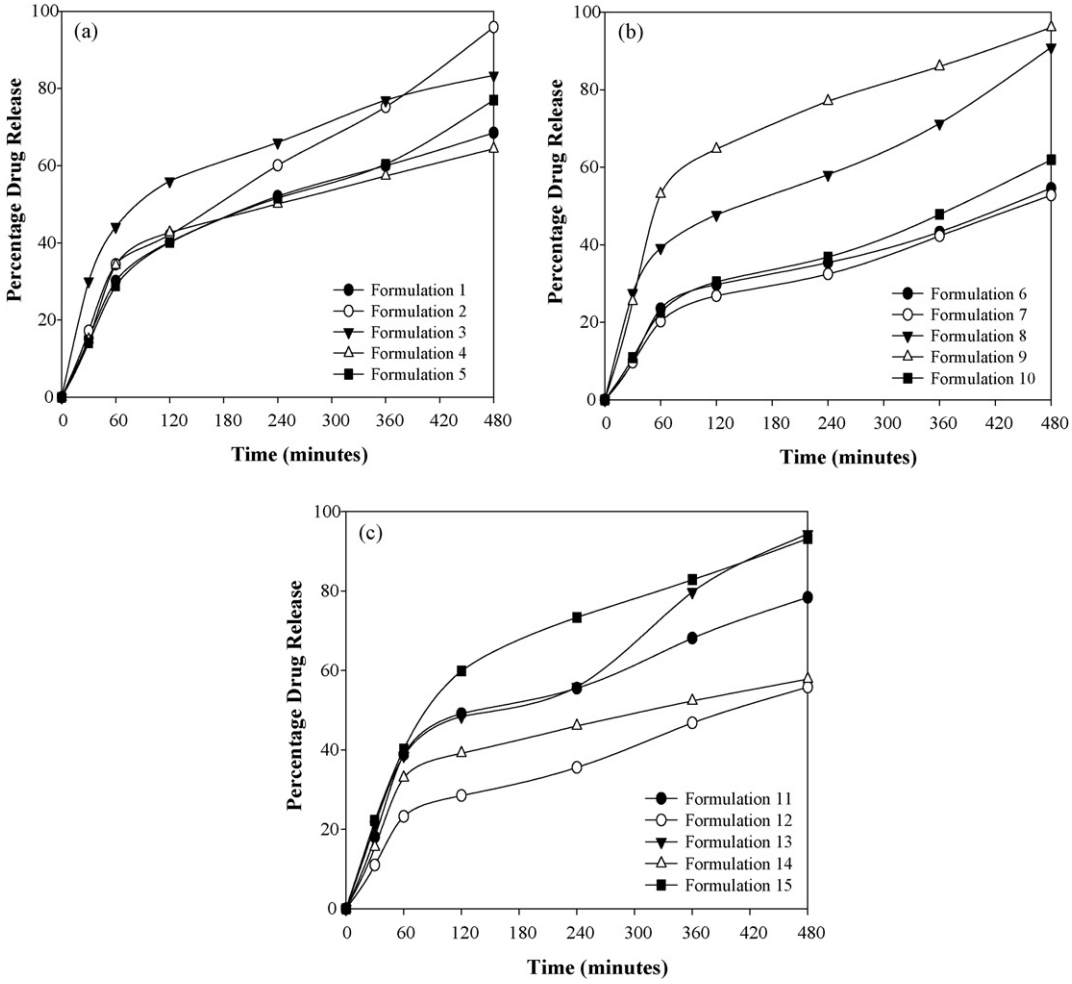

Fig. 1. Drug release profiles for the 15 formulations in simulated saliva (pH, 6.8) prior to optimization ($n = 3$ and SD $\leq 4.56\%$ in all cases).

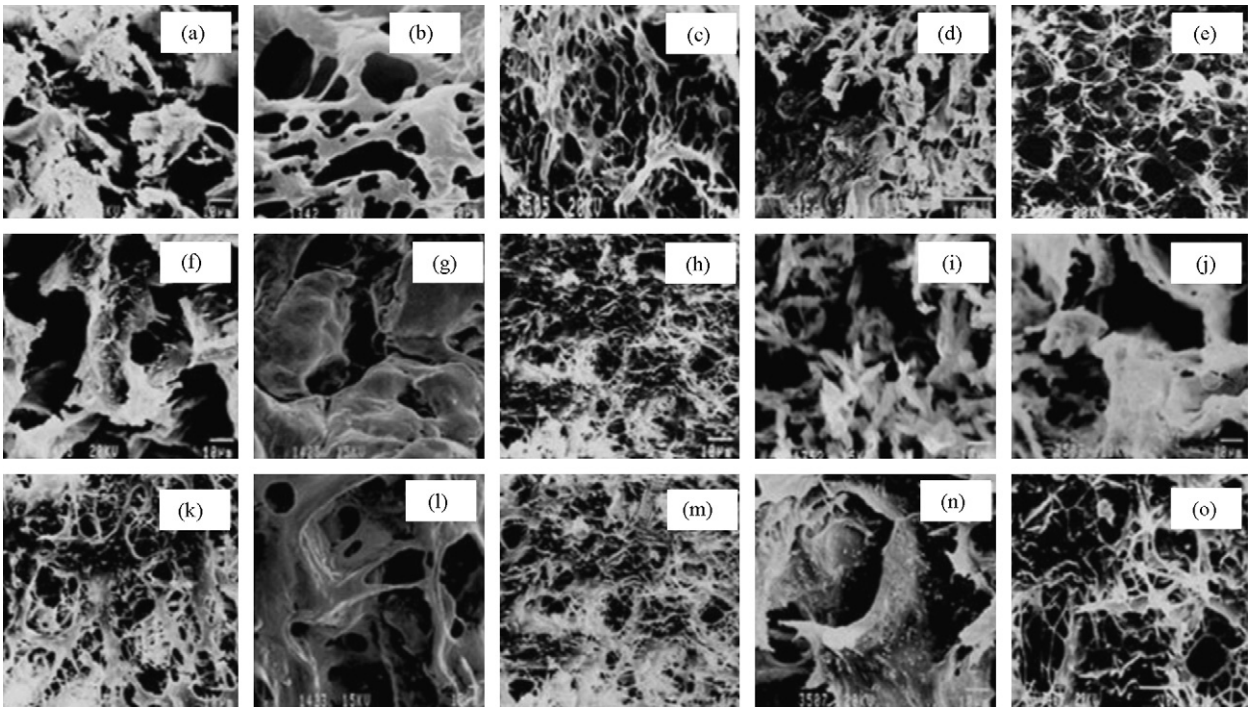

Fig. 2. Scanning electron micrographs of the P-EAMs showing the diversity of pore structures, distributions and interconnectors (magnification 1000×).

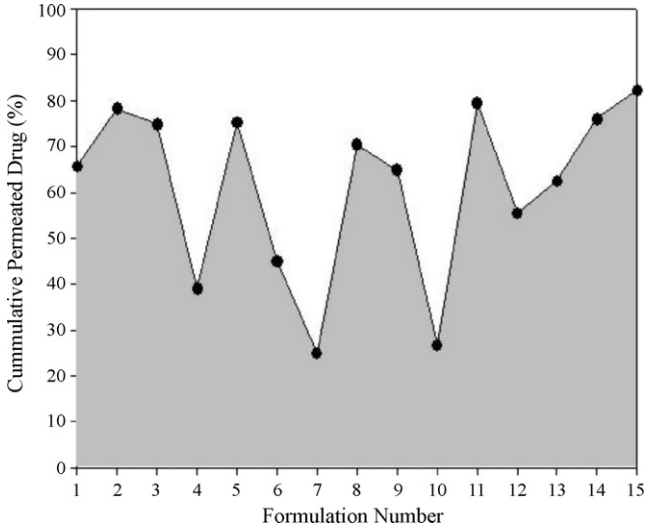

Fig. 3. Area plot presenting the cumulative quantity of phenytoin sodium that diffused through the porcine buccal mucosa into the receptor compartment in 8 h ($n = 3$ and SD ≤ 1.41% in all cases).

with formulations that showed rigid interconnectors (Fig. 3f, g, j and n) representing formulations 6, 7, 10 and 14, respectively in which case drug release was slower with <65% liberated over 8 h (Fig. 2). Consequently, the pore interconnectors functioned as barriers within the porous matrices and played a role of regulating matrix hydration, disentanglement, diffusion of drug and erosion.

The quantity of pore-forming agent added when preparing the matrices was noted to have had a significant influence on the exhibited porous structures of the matrices. In addition, ethanol was a more potent pore-forming agent than water with respect to this study as a slight increment in the volume of ethanol resulted in visible changes in pore structure (i.e. enhanced porosity). For instance, formulations 2, 3, 4, 5, 6, 8, 11, 13 and 15 containing the highest levels of ethanol (11 and 13 mL) displayed larger and higher volume of pores (Fig. 2b–f, h, k, m and o, respectively) when compared with formulations 7, 12 and 14 (Fig. 3g, l and n) with highest volume of water (30 mL) giving rise to lower volumes of pores distribution. In addition, formulations 1, 9 and 10 (Fig. 3a, i and j) are exceptions to this trend and this may be due to other physicochemical influences of the co-particulate components on the sublimation of the frozen pore-forming agents from the matrices during the process of lyophilization.

3.4. Drug-loading capacity of the P-ECMs

Generally, effective drug-loading was attained with values ranging from 53.14 ± 2.19 to 99.02 ± 0.74% (Table 6). Drug-loading does not appear to follow on any particular trend as regards the level of solute or solvent compositions for each formulation. Overall, it can be proposed that the extent of drug loading could be related to the degree of miscibility of the drug molecules with the respective homogenous blends.

3.5. Extent of permeation of drug molecules through the porcine buccal mucosa

The capabilities of the formulations to initiate and sustain the permeation of phenytoin sodium molecules through the porcine buccal tissue was observed and results illustrated in Figs. 3 and 4 as cumulative drug permeated (%) and drug flux (mg cm^{-2} min^{-1}), respectively over 8 h for the 15 formulations. The drug flux values were calculated using Eq. (2). Overall, the formulations showed

Table 6
Percentage drug loading capacity for the 15 formulations.

Formulation	% Drug-Loading Capacity (DLC) ± SD[a]
1	58.60 ± 1.68
2	80.54 ± 0.33
3	95.14 ± 2.54
4	99.10 ± 0.49
5	94.64 ± 3.77
6	99.02 ± 0.21
7	97.54 ± 1.03
8	66.83 ± 2.24
9	83.27 ± 3.34
10	79.28 ± 2.27
11	94.85 ± 1.98
12	98.64 ± 0.88
13	53.14 ± 2.55
14	81.38 ± 1.67
15	79.18 ± 1.09

[a] SD: standard deviation.

diverse permeation-enhancing capabilities as different amounts of drug molecules passed through the tissue within the set experimentation time (Fig. 3).

Different levels of each permeation enhancer (SP 80 and menthol) displayed extensive co-interactive, combined influences but a relatively coherent general pattern of impact on permeation initiation and maintenance was noticed. Overall, the permeation enhancers were observed to be most efficient at mid to low factor levels (Tables 1 and 2) while the converse is applicable to the highest factor levels of the enhancers.

The values of cumulative flux, i.e. the rate of drug permeation over the surface area, differed in the formulations, which may be due to complex interactions between the permeation enhancers as well as other components within each matrix. An independent, non-linear relationship was observed between the quantity of drug that permeated through the tissue into the recipient compartment and the drug flux (Fig. 4). In other words, the rate at which the drug molecules permeate through the tissue (flux) was not a determining factor for the amount of drug that was eventually detected in the recipient compartment or the quantity that permeated through the tissue specimen.

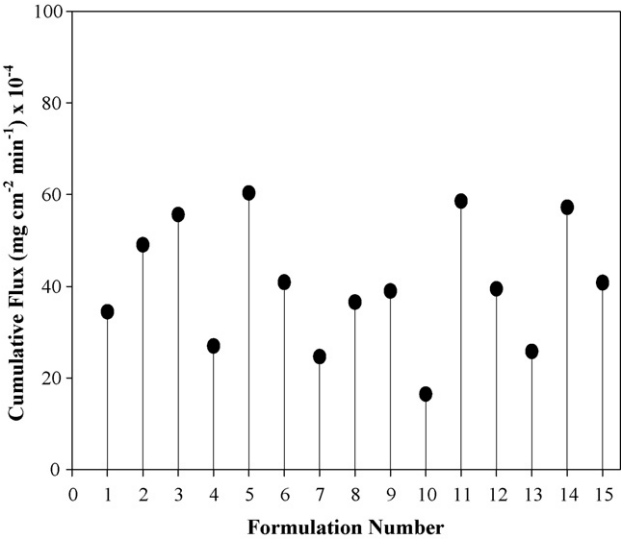

Fig. 4. Cumulative steady state flux values computed at 480 min for the 15 formulations ($n = 3$ and SD ≤ 1.99×10^{-4} mg cm^{-2} min^{-1} in all cases).

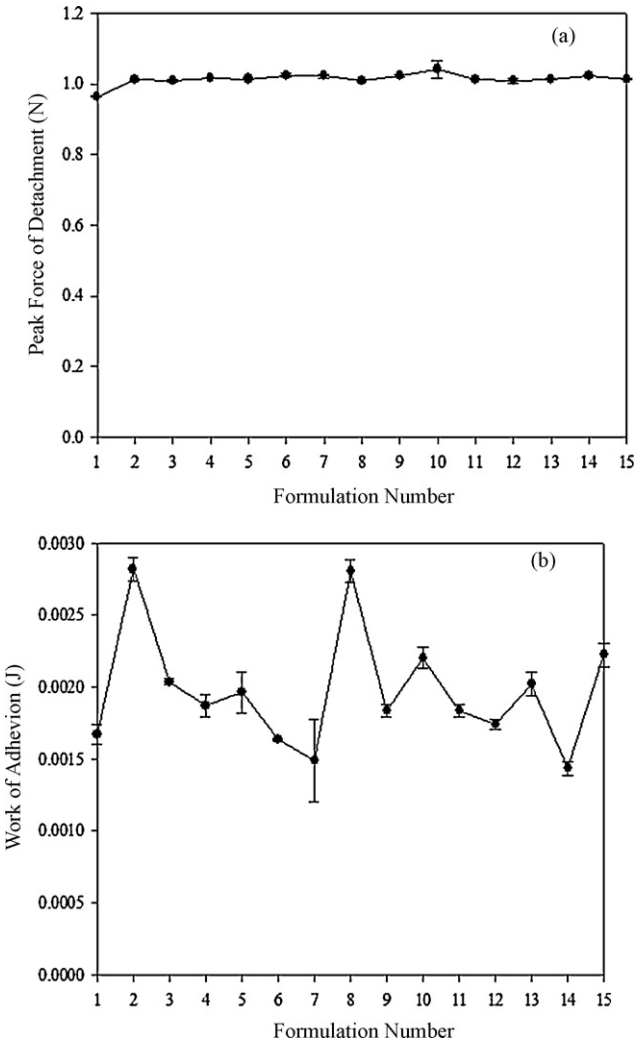

Fig. 5. Numerical values of: (a) peak detachment force in Newton and (b) work or energy of bio-adhesion in Joules of the 15 formulations ($n = 3$ and in all cases).

3.6. Ex vivo bio-adhesion testing

The capability of the formulations to adhere to the model buccal mucosal tissue was made evident by the values obtained for the peak force of detachment (F_{det}) (0.9636 ± 0.015 to 1.042 ± 0.025 N) and work of adhesion (ω_{adh}) (0.0014 ± 0.00005 to 0.0028 ± 0.00008 J) (Fig. 5). No specific trend was observed with the differences in the quantities of the bioadhesive components (gelatin and Carbopol® 974) included during the preparation of the P-EAMs. It can be proposed that gelatin and Carbopol® 974 complemented each other in influencing the overall bioadhesive characteristics of the matrices. This explains why all formulations showed a level bioadhesive competence. Additionally, particular patterns directly or inversely relating F_{det} to ω_{adh} were absent implying that the F_{det} did not specifically influence the values of ω_{adh}. This may be attributable to the fact that the energy expended during the process of bioadhesion or the force of detachment are extensively influenced by the inter-surface electrostatic interactions between the different matrices, buccal mucosal tissue, and simulated saliva that may be dependent on the proportions of the bioadhesive agents as well as other compounds present within each matrix.

Table 7
Levels of solute and solvent components for the fabrication of the optimized P-EAM.

Composition	Optimized level
ACD[a]	0.00 mg/20 mL
ECD[b]	4.50 mg/9 mL
SP 80[c]	0.50 mL

ACD: 0 – PVA (800 mg) + HEC (350 mg) + GEL (400 mg) + CARB974 (100 mg) + DW (30 mL).
ECD: 4.5 – CHTS (362.5 mg) + MS (312.5 mg) + MTH (275 mg) + ETH 10 (550 mg) + EtOH (9 mL).
[a] Aqua-based co-particulate dispersion.
[b] Ethanol-based co-particulate dispersion.
[c] Span 80.

3.7. Quantitative porositometric analysis of the matrices

Porosimetric analysis quantified the total pore volume, surface area, and average pore diameter. This investigation further validated the findings depicted by the generated SEM micrographs (Fig. 2) for each formulation. Average pore diameters ranged between 40 and 100 Å. The cumulative pore volume, as a measure of pore distribution, had values from 5×10^{-4} to 6.5×10^{-3} cm^3/g and the cumulative surface area ranged from 28–800 cm^2/g. The above-mentioned numerical measures demonstrate that the performance of the P-EAM was highly dependent on the pore structure, diameter, and volume of pore distribution which also signifies the integrity and configuration of the interconnectors as well as the surface area. These parameters vary for each formulation and this is observed to have a significant impact on their displayed physicochemical properties. In addition, the range of pore sizes indicated that the 15 formulations were mesoporous in nature. Fig. 6(a)–(c), respectively illustrate the average pore diameter, cumulative pore volume and surface area measured for the 15 experimental design formulations.

3.8. Preparation and testing of the optimized formulation

Based on the optimization procedure, a formula was developed for the fabrication of the optimized formulation (Table 7). The fabricated optimized formulation was assessed to ascertain the existence of a correlation between the experimentally and fitted data as well as confirming the suitability of the experimental design employed. The formulation was assessed based on its drug loading capacity, bioadhesive strength, mean dissolution time (from drug release) and cumulative *ex vivo* drug permeation. Drug release and *ex vivo* permeation from this specialized matrix was targeted at 8 h to aid convenience during use by a patient.

The statistical significance measured as *p-values* ≤ 0.05 and $R^2 > 0.90$ displayed (Table 4) by the response parameters indicate that the different levels of the independent formulation variables employed in constructing the optimized P-EAM had noticeable influence on its overall performance. A high degree of correlation between the experimental and statistically fitted values based on the ANOVA was observed for each selected response parameter (Table 8). This outcome further reveals the stability and adequacy

Table 8
Comparison of the fitted and experimental values of the response parameter to assess the efficiency of the experimental design for formulation optimization.

Response parameters	Fitted response	Experimental response
Mean dissolution time (MDT) (min)	90.00	94.10 ± 2.90
Drug loading capacity (DLC) (%)	100.00	99.72 ± 3.56
Bioadhesive strength (BA) (N)	1.20	1.18 ± 0.05
Cumulative drug permeation (PA) (%)	90.00	85.68 ± 3.33

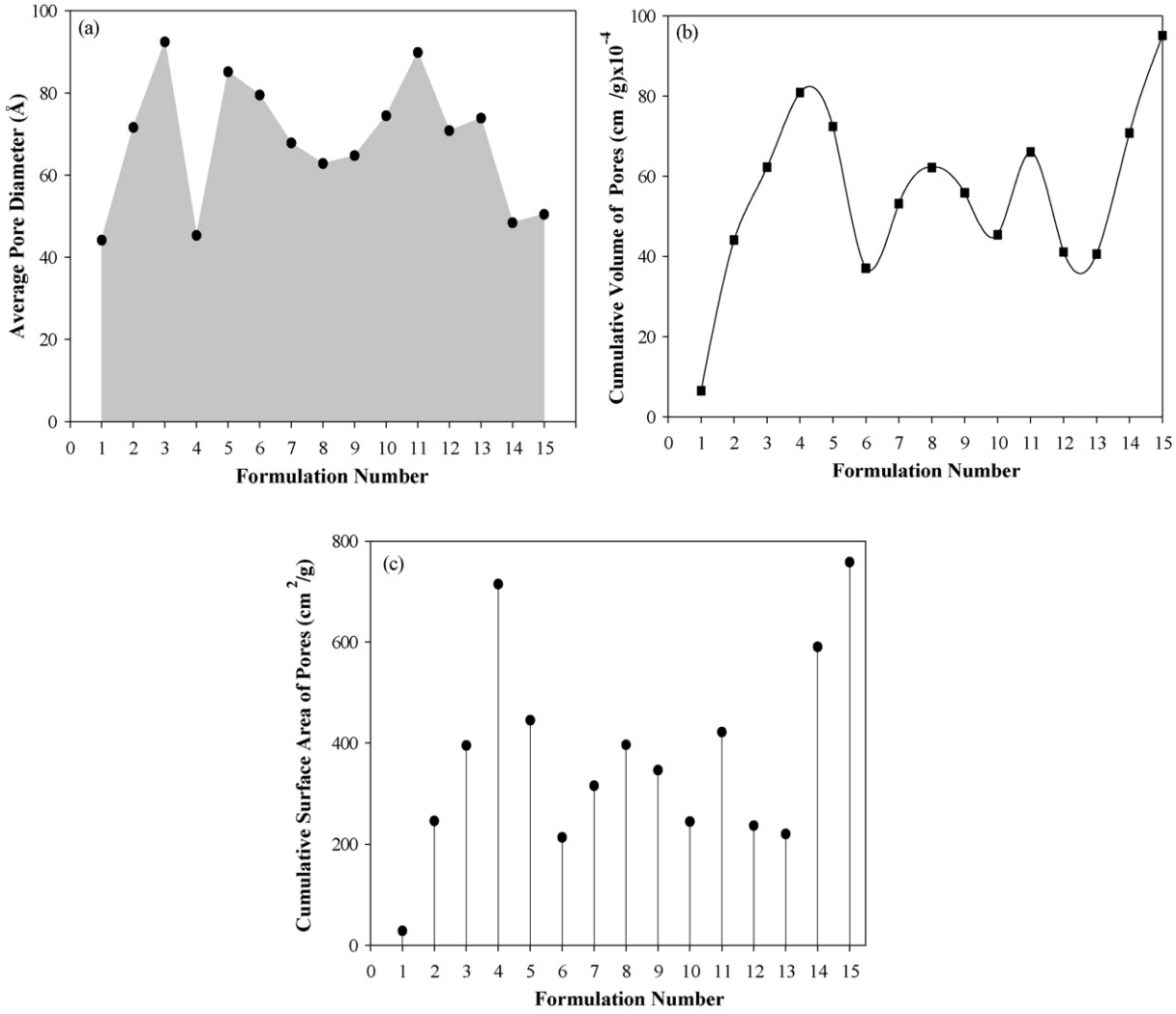

Fig. 6. (a) Average pore diameters showing their mesoporous nature (SD ≤ 5 Å in all cases), (b) cumulative volume of pores (SD ≤ 7.74×10^{-4} cm^3/g in all cases) and (c) cumulative surface area of pores (SD ≤ 20.97 cm^2/g in all cases) for the 15 formulations ($n = 3$ in all cases).

of the statistical design employed for generating the desired optimized formulation.

The optimized P-EAM retained the mesoporous structure of the experimental design formulations with a pore diameter of 86.01 ± 4.04 Å. Representative drug release and *ex vivo* drug permeation profiles of the optimized formulation are shown in Fig. 7(a) and (b), respectively. Optimized formulation displayed the potential to consistently release drug molecules in a steady state, controlled manner over 480 min. Furthermore, the formulation showed the capability to consistently initiate and sustain the per-

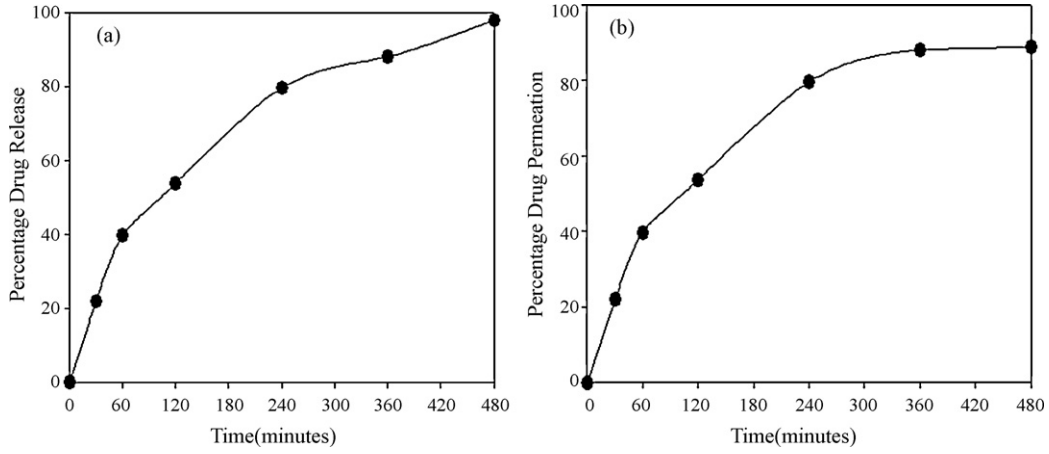

Fig. 7. Cumulative of phenytoin sodium (a) in simulated saliva, pH 6.8 and (b) by *ex vivo* permeation through the porcine buccal mucosa over 480 min ($n = 3$ and SD ≤ 10.77% in all cases).

meation of drug molecules from the donor compartment through the model buccal mucosal tissue into the receiving compartment of the Franz diffusion cells over the period of 480 min. A close to linear, sustained permeation of the drug molecular species was observed over time (Fig. 7(b)) suggesting passive diffusion initiated and maintained by the P-EAM formulation to be the possible mechanism of drug permeation. Also, the consistent increment in the percentage of drug released over time may indicate that the mucosal sites for permeation were not saturated over the period of exposure to the drug loaded optimized formulation.

The drug permeation pattern (Fig. 7(b)) may be described as biphasic as a rapid, linear increase in drug permeation levels up to the 4th hour was observed, followed by slight increments resembling a plateau up to the 8th hour. This observed trend may be of an advantage as initial rapid linear increase in drug permeation levels can initiate pharmacotherapeutic actions and relief to the patient while the second phase maintains the plasma levels of drug molecules thereby enhancing reduction of dosage frequencies and possibly enhancing patient compliance.

4. Conclusion

This study provides valuable information that can be employed in developing novel porosity-enabled matrices for application in transmucosal drug delivery. The Box–Behnken quadratic design employed for the fabrication of the P-EAMs revealed the impact of porosity (pore structure, interconnectors, pore width or diameter, and pore volume of distribution) on their physicochemical properties due to the variations in the levels of independent variables employed during the process of fabrication. Interphase, co-particulate, co-solvent, homogenization coupled with lyophilization, proved to be efficient methods for construction of the P-EAMs. This indicates the efficiency of these methods as matrices retained the contributing effects of individual chemical compounds that comprised each formulation. The distinct flexible physicochemical characteristics observed with the formulations imply that the P-EAMs explored in this investigation can be described as versatile systems which make them attractive for the adapted invention and construction of novel drug delivery systems. Statistical analysis of data further confirmed the dependency of the measured physicochemical response parameters on the independent variables or factor levels ($p\text{-}values \leq 0.05$). As part of mechanistic characterization, an optimized P-EAM formulation was constructed based on the information generated. Physicochemical parameters which are related to the intended application of the formulation and influenced by matrix porosity were selected for the formulation optimization process. These response parameters included bio-adhesion, drug-loading capacity, drug release and cumulative permeation. The experimental and fitted values generated were closely related, indicating the adequacy and reliability of the statistical design employed. Conclusively, an optimized P-EAM formulation was successfully designed and the investigated physicochemical properties revealed the potential of this matrix to be applied for sustained transbuccal drug delivery.

Acknowledgements

This work was funded by BioPAD (SA), a Biotechnology Regional Innovation Centre and an initiative of the Department of Science and Technology, South Africa and a scholarship awarded by the Medical Research Council of South Africa.

References

Ahmed, A., Bonner, C., Dessai, C., 2002. Bioadhesive microdevices with multiple reservoirs: a new platform for oral drug delivery. J. Control. Release 81, 291–306.

Åkerman, S., Viinikk, P., Svarfvar, B., Jarvinen, K., Kontturi, K., Nasman, J., 1998. Transport of drugs across porous ion exchange membranes. J. Control. Release 50, 153–166.

Alur, H.H., Johnston, T.P., Mitra, A.K., 2001. Encyclopedia of pharmaceutical technology. In: Superbrick, J., Boylan, J.C. (Eds.), Peptides and Proteins: Buccal absorption, vol. 20 (3), pp. 193–218.

Alvarez-Núñez, F.A., Yalkowsky, S.H., 1999. Buffer capacity and precipitation control of pH solubilzed phenytoin formulations. Int. J. Pharm. 195, 45–49.

Bromberg, L.E., Buxton, D.K., Friden, P.M., 2001. Novel periodontal drug delivery system for the treatment of periodontitis. J. Control. Release 71, 251–259.

Chien, Y.W., 2006. Novel drug delivery systems. Drugs and the Pharmaceutical Sciences, vol. 50, pp. 197–200.

Chu, L., Liang, Y., Chen, W., Ju, X., Wang, H., 2004. Preparation of glucose-sensitive microcapsules with porous membrane and functional gates. Colloids Surf. B 37, 9–14.

Consuelo, D.D., Pizzolato, G.P., Falson, F., Guy, R.H., Jacques, Y., 2005. Evaluation of pig esophageal mucosa as a permeability barrier model for buccal tissue. J. Pharm. Sci. 94, 2777–2788.

Darwish, I.A., El-Massik, M.A., Hassan, E.E., El-Khordagui, L.K., 1996. Assessment of a hydroalcholic surfactant solution as a medium for the dissolution testing of phenytoin. Int. J. Pharm. 140, 25–32.

Giannola, L.I., De Caro, V., Giandalia, G., Siragusa, M.G., Tripodo, C., Florena, A.M., Campisi, G., 2007. Release of naltrexone on buccal mucosa: permeation studies, histological aspects and matrix system design. Eur. J. Pharm. Biopharm. 67, 425–433.

Hoa, M.L.K., Lu, M., Zhang, Y., 2006. Preparations of porous materials with ordered hole structure. Adv. Colloid Interf. 121, 9–23.

Kim, H., Knowles, J.C., Kim, H., 2004. Hydroxyapatite/poly(e-caprolactone) composite coatings on hydroxyapatite porous bone scaffold for drug delivery. Biomaterials 25, 1279–1287.

Korsmeyer, R.W., Gurny, R., Doelker, E., Buri, P., Peppas, N.A., 1983. Mechanisms of solute release from porous hydrophilic polymers. Int. J. Pharm. 15, 25–35.

Li, Z., Wen, L., Shao, L., Chen, J., 2004. Fabrication of porous hollow silica nanoparticles and their applications in drug release control. J. Control. Release 98, 245–254.

Matthews, K.H., Stevens, H.N.E., Auffret, A.D., Humphrey, M.J., Eccleston, G.M., 2005. Lyophilised wafers as a drug delivery system for wound healing containing methylcellulose as a viscosity modifier. Int. J. Pharm. 289, 51–62.

Miao, X., Hu, Y., Liu, J., Wong, A.P., 2004. Porous calcium phosphate ceramics prepared by coating polyurethane foams with calcium phosphate cements. Mater. Lett. 58, 397–402.

Moon Suk, K., Kwang Su, S., Hoon, H., Sun Kyung, K., Gilson, K., Hai Bang, L., 2005. Sustained release of bovine serum albumin using implantable wafers prepared by MPEG-PLGA diblock copolymers. Int. J. Pharm. 304, 165–177.

Netz, D.J.A., Sepulveda, P., Pandolfelli, V.C., Spadaro, A.C.C., Alencastre, J.B., Bentley, M.V.L.B., Marchetti, J.M., 2005. Potential use of gelcasting hydroxyapatite porous ceramic as an implantable drug delivery system. Int. J. Pharm. 213, 117–125.

Orive, G., Hernandez, R.M., Gascon, A.R., DominguezGily, A., Pedraz, J.L., 2003. Drug delivery in biotechnology: present and future. Curr. Opin. Biotechnol. 14, 659–664.

Park, Y.J., Nam, K.H., Ha, S.J., Pai, C.M., Chung, C.P., Lee, S.J., 1997. Porous poly(L-lactide) membranes for guided tissue regeneration and controlled drug delivery: membrane fabrication and characterization. J. Control. Release 43, 151–160.

Patel, R., Pillay, V., Choonara, Y.E., Govendar, Thirunula, 2007. A novel cellulose-based hydrophilic wafer matrix for rapid bioactive delivery. J. Bioact. Compat. Pol. 22, 119–142.

Peh, K.K., Wong, C.F., 1999. Polymeric films as vehicle for buccal delivery: swelling, mechanical and bioadhesive properties. J. Pharm. Pharm. Sci. 2, 53–61.

Pellock, J.M., Smith, M.C., Cloyd, J.C., Uthman, B., Wilder, B.J., 2004. Extended-release formulations: simplifying strategies in the management of antiepileptic drug therapy. Epilepsy Behav. 5, 301–307.

Pillay, V., Fassihi, R., 1998. Evaluation and comparison of dissolution data derived from different modified release dosage forms: an alternative method. J. Control. Release 55, 45–55.

Ponchel, G., Montisci, M., Dembri, A., Durrer, C., Duchêne, D., 1997. Mucoadhesion of colloidal particulate systems in the gastro-intestinal tract. Eur. J. Pharm. Biopharm. 44, 25–31.

Portero, A., Teijeiro-Osorio, D., Alonso, M.J., Remunan-Lopez, 2007. Development of chitosan sponges for buccal administration of insulin. Carbohyd. Polym. 68, 617–625.

Rinaki, E., Dokoumetzidis, A., Macheras, P., 2003. The mean dissolution time depends on the dose/solubility ratio. Pharm. Res. 20, 406–408.

Rodríguez-Lorenzo, L.M., Ferreira, J.M.F., 2004. Development of porous ceramic bodies for applications in tissue engineering and drug delivery systems. Mater. Res. Bull. 39, 83–91.

Sher, P., Ingavle, G., Ponrathnam, S., Pawar, A.P., 2007. Low density porous carrier drug absorption and release study by response surface methodology using different solvents. Int. J. Pharm. 331, 72–83.

Smart, J.D., 2005. The basics and underlying mechanisms of mucoadhesion. Adv. Drug Deliv. Rev. 57, 1556–1568.

Sohier, J., Vlugt, T.J.H., Cabrol, N., Van Blitterswijk, C., de Groot, K., Bezemer, J.M., 2006. Dual release of proteins from porous polymeric scaffolds. J. Control. Release 111, 95–106.

Sudhakar, Y., Kuotsu, K., Bandyopadhyay, A.K., 2006. Buccal bioadhesive drug delivery—a promising option for orally less efficient drugs. J. Control. Release 114, 15–40.

Tang, C., Yin, C., Pei, Y., Zhang, M., Wu, L., 2005. New superporous hydrogels composites based on aqueous carbopol® solution (SPHCcs): synthesis, characterization and in vitro bioadhesive force studies. Eur. Polym. J. 41, 557–562.

Tao, S.L., Desai, T.A., 2003. Microfabricated drug delivery systems: from particles to pores. Adv. Drug Deliv. Rev. 55, 315–328.

Van der Bijl, P., Van Eyk, A.D., Thompson, I.O.C., Stander, I.A., 1998. Diffusion rates of vasopressin through human vaginal and buccal mucosa. Eur. J. Oral. Sci. 106, 958–962.

Van Eyk, A.D., Thompson, I.O.C., 1998. Effects of freezing on the permeability of human buccal and vaginal mucosa. S. Afr. J. Sci. 94, 499–502.

Van Eyk, A.D., Van der Bijl, 2004. Comparative permeability of various chemical markers through human vaginal and buccal mucosa as well as porcine buccal and mouth floor mucosa. Arch. Oral. Biol. 49, 387–392.

Wang, X., Patsalos, P.N., 2003. A comparison of central brain (cerebrospinal and extracellular fluids) and peripheral blood kinetics of phenytoin after intravenous phenytoin and fosphenytoin. Seizure 12, 306–330.

Wang, Y., Chang, H., Wertheim, D.F., Jones, A.S., Jackson, C., Coombes, A.G.A., 2007. Characterisation of the macroporosity of polycaprolactone-based biocomposited and release kinetics for drug delivery. Biomaterials 28, 4619–4627.

Zhang, Y., Wang, Y., Shi, B., Cheng, X., 2007. A platelet-derived growth factor releasing chitosan/coral composite scaffold for periodontal tissue engineering. Biomaterials 28, 1515–1522.